

Electric and Magnetic Field Studies on Rodlike fd-Virus Suspensions

C. Martin,^{*,†} H. Kramer,[‡] C. Johner,[†] B. Weyerich,[†] J. Biegel,[†] R. Deike,[†] M. Hagenbüchle,[†] and R. Weber[†]

Fakultät für Physik, Universität Konstanz, 78434 Konstanz, Germany, and
Max-Planck-Institut für Festkörperforschung, Hochfeld-Magnetlabor, Grenoble, France

Received September 6, 1994; Revised Manuscript Received February 9, 1995[®]

ABSTRACT: The electrical and optical properties of rodlike fd-virus particles ($L = 880$ nm, $D = 9$ nm) are investigated by magnetic and electric birefringence experiments and supplemented by electric field light-scattering measurements. In aqueous suspension the fd-virus particles are negatively charged and surrounded by diffuse counterion clouds. The examinations are performed at very low ionic strength (10^{-6} M). Under these conditions a liquid crystalline phase already occurs at fd-particle concentrations above 0.6 mg/mL. In magnetic fields the rodlike fd-virus is aligned parallel to the magnetic field due to its diamagnetic anisotropy. Almost complete particle alignment in magnetic fields is obtained for liquid crystalline samples, and the saturation value of the birefringence is determined. The application of electric fields results in a polarization of the counterion clouds and a statistical orientation of the dispersed particles. In low electric fields Kerr behavior is found, providing the electric anisotropy $\Delta\alpha_{el}$ of a single rod. At higher electric fields the diffuse Debye cloud is partly stripped away and a complete particle orientation is hindered. Electric field light-scattering investigations yield quantitatively the decrease of the electric anisotropy $\Delta\alpha_{el}$ in high electric fields.

1. Introduction

We study the orientational behavior of the rodlike bacteriophage fd in aqueous solution in external magnetic and electric fields. The fd-virus has a length of $L = 880 \pm 20$ nm,^{1–4} a diameter of $D = 9 \pm 2$ nm, and a molecular weight of 16.4×10^6 Dalton.² Due to its molecular structure the fd-virus is optical and diamagnetic anisotropic.⁴ On its surface approximately 10^4 ionizable acid groups are located.⁵ In aqueous suspensions the virus is therefore negatively charged and surrounded by a diffuse Debye counterion cloud. In this paper we are interested in suspensions of very low ionic strength (10^{-6} M) leading to large counterion clouds of several hundred nanometers. The strong electrostatic interparticle interaction causes a liquid crystalline phase at relatively small particle concentrations of $c \approx 0.6$ mg/mL.⁶

The molecular structure of the fd-virus is well understood.^{1–4,7,8} Nevertheless there exists a discrepancy about its optical anisotropy which is directly related to the saturation value of birefringence experiments.⁴ Complete particle alignment in a magnetic field is only obtained for nematic liquid crystalline samples. A previous publication of Tang and Fraden⁹ shows evidence of saturation of birefringence, but their value is much lower than the one found by Torbet and Maret.⁴ Both saturation values were obtained at particle concentrations above 11 mg/mL and at high ionic strengths. In the present study we measured the saturation value $\Delta n_{sat}/c$ in a magnetic field at minimal ionic strength (10^{-6} M) and a much lower particle concentration of $c = 0.8$ mg/mL.

Our previous electric birefringence examinations⁶ have shown that the particles are oriented by an induced dipole in an external electric field. The induced dipole originates from a deformation of the counterion cloud. Therefore the extension of the counterion cloud strongly contributes to both the interaction of a single

fd-virus particle with the external electric field and the interparticle interaction of the rods. The measured saturation for electric birefringence was far below the saturation value given by Torbet and Maret of $\Delta n_{sat}/c = 6.0 \times 10^{-5}$ mL/mg⁴ and even below the value estimated by Tang and Fraden of about $\Delta n_{sat}/c = (2.4–2.7) \times 10^{-5}$ mL/mg.⁹ We interpreted that deviation of the saturation value in an electric field as a stripping of the diffuse counterions away from the electrostatic influence of the central rod in high electric fields which is correlated to a decrease of the electric polarizability of a rod.⁶ This effect was theoretically predicted by several authors.^{10–12}

The relative change of the scattered light intensity $\Delta I/I_0$ in an electric field yields information about the orientation of the suspended particles with respect to the field direction. For the first time we measured the dependence of electric anisotropy $\Delta\alpha_{el}$ on the electric field strength with the method of electric field light scattering.^{13,16} In that way we can experimentally support the theoretical considerations concerning the polarization of the ion atmosphere in high electric fields.

2. Theory

2.1. Order Parameter and Birefringence. U_{orient} is the potential energy of a single rod in an external field. In the case of the fd-virus particles which are purely diamagnetic and without a permanent electric dipole moment U_{orient} can be written in the following ways. In an external magnetic field it is given by⁴

$$U_{orient} = -\frac{\Delta\chi B^2}{2\mu_0} \cos^2 \theta \quad (1)$$

$\Delta\chi = \chi^{\parallel} - \chi^{\perp}$ is the anisotropy of the diamagnetic susceptibility of a single rod, B is the magnetic field, μ_0 is the permeability of free space, and θ is the angle between the rod length axis and the external field. In an external electric field U_{orient} is expressed by¹⁶

[†] Universität Konstanz.

[‡] Max-Planck-Institut für Festkörperforschung.

[®] Abstract published in *Advance ACS Abstracts*, March 15, 1995.

$$U_{\text{orient}} = -\frac{\Delta\alpha_{\text{el}}E^2}{2} \cos^2 \theta \quad (2)$$

$\Delta\alpha_{\text{el}} \equiv \alpha_{\text{el}}^{\parallel} - \alpha_{\text{el}}^{\perp}$ is the electric anisotropy of a single rod, and E the effective electric field strength. The parameter γ is defined as $\gamma \equiv \Delta\alpha_{\text{el}}E^2/2k_{\text{B}}T$ and is proportional to the ratio of the orientation energy U_{orient} and the thermal energy $k_{\text{B}}T$.

The external field causes an anisotropic orientation distribution of the rods, and the suspension becomes optically anisotropic (birefringent). The order parameter $\Phi(U_{\text{orient}}, T)^{17}$ indicates the degree of orientation of the suspended particles:

$$\phi(U_{\text{orient}}, T) = 2\pi \int_0^\pi d\theta \sin \theta \left[\frac{3 \cos^2 \theta - 1}{2} \right] f(\theta) \quad (3)$$

In the case of an electric field the order parameter is solely determined by the field parameter γ .

In the steady-state regime the orientation distribution function $f(\theta)$ is described by a Boltzmann distribution:

$$f(\theta) = \frac{e^{-U_{\text{orient}}/k_{\text{B}}T}}{2\pi \int_0^\pi d\theta \sin \theta e^{-U_{\text{orient}}/k_{\text{B}}T}} \quad (4)$$

The birefringence Δn_0 is directly correlated to the order parameter:

$$\Delta n_0 = \Delta n_{\text{sat}} \Phi(U_{\text{orient}}, T) \quad (5)$$

where Δn_{sat} is the saturation birefringence for completely aligned rods determined by the optical anisotropy $\Delta\alpha_{\text{opt}}$ of a single particle.⁴

For $\gamma \leq 1$ the order parameter $\Phi(\gamma)$ can be expanded and the birefringence Δn_0 is given by the Kerr law:¹⁷

$$\Delta n_0 = \frac{\Delta n_{\text{sat}} \Delta\alpha_{\text{el}}}{15k_{\text{B}}T} E^2 \quad (6)$$

2.2. Electric Field Light Scattering. In a static light-scattering experiment the time-averaged scattered intensity $I(q)$ of a disperse system of N monodisperse interacting particles is measured. The intensity of the scattered light within the Rayleigh–Gans–Debye approximation (RGD) can be expressed by the one-particle form factor $P(q)$ and the static structure factor $S(q)$:^{13–15}

$$I(q) \propto NP(q)S(q) \quad (7)$$

Here, the form factor $P(q)$ describes the intramolecular interferences, and the contributions from intermolecular correlations are given by the static structure factor $S(q)$. The magnitude of the scattering vector q is defined as

$$q = \frac{4\pi n}{\lambda} \sin\left(\frac{\vartheta}{2}\right) \quad (8)$$

where λ is the laser wavelength of the incident light, n is the refractive index of the aqueous suspension ($n = 1.33$), and ϑ is the angle of observation.

The application of electric fields to suspensions of electrically anisotropic macromolecules results in a change of the angular distribution of the scattered light. The relative intensity change of light scattered by anisodiametric particles in an external electric field is defined by¹⁶

$$\frac{\Delta I}{I_0} = \frac{I_{\text{E}}(q) - I_0(q)}{I_0(q)} \quad (9)$$

$I_{\text{E}}(q)$ denotes the steady-state value of the scattered light intensity when the particles are subjected to an electric field, and $I_0(q)$ is the scattered intensity of the isotropically oriented rods without an external field.

Considering only the contributions from the change of the intramolecular interferences, i.e. the change of the form factor $P(q, \gamma)$ due to particle alignment in an external electric field, a theoretical treatment of the relative change of the scattered light $\Delta I(q, \gamma)/I_0$ was derived by Stoimenova¹⁸ for particles within the Rayleigh–Gans–Debye approximation.^{13,19} In the present study we suppress the influence of the static structure factor $S(q)$ by fixing the detector at a high scattering angle ($\vartheta = 140^\circ$) where the interparticle interferences do not contribute to the scattered light intensity $I(q)$, i.e. $S(q) \approx 1$.^{14,15} The fd-virus particles are modeled as monodisperse rigid rods of length L^{20} and vanishing diameter. It is further assumed that in the case of light scattering the optical anisotropy of the fd-particles is negligible. The suspension should be sufficiently diluted and therefore free of multiple scattering effects. The incident light is plane polarized. In the experimental setup the electric field is fixed perpendicular to the plane of observation. The steady-state value of the relative change of the scattered light intensity $\Delta I/I_0$ for infinitely thin rods in an external field is expressed by^{13,18}

$$\begin{aligned} \frac{\Delta I}{I_0} = & \frac{16\pi}{P_0(q)T_n} \left\{ \sum_{p=0}^{\infty} \frac{\gamma^{2p}(4p-1)!!}{(2p)!(4p)!!} \sum_{m=0}^{\infty} \xi_{p,m}(qL)^{2m} [1 + \zeta_{p,m}\gamma] \right\} - 1 \\ \xi_{p,m} = & \frac{(-1)^m(2m-1)!!(4p)!!}{2(2m+2)!(2m+4p+1)!!} \\ \zeta_{p,m} = & \frac{(4p+1)}{(2p+1)(2m+4p+3)} \end{aligned} \quad (10)$$

$P_0(q)$ is the form factor for isotropically oriented rods.²¹ The normalizing factor $T_n(\gamma) = 2\pi \int_0^\pi d\theta \sin \theta \exp(\gamma \cos^2 \theta)$ was tabulated by Dawson;²² it can easily be calculated numerically. Numerical calculations of eq 10 fit the measured data at higher scattering angles where interparticle interferences can be neglected using respectively γ or $\Delta\alpha_{\text{el}}$ as a fit parameter. A systematic study of the q dependence of the electric field light scattering is published elsewhere.¹³

For small electric field strengths at a low degree of orientation eq 10 corresponds to the formulas derived by Wippler.²³ $\Delta I/I_0$ in the Kerr regime is directly related to the electric anisotropy of a single particle²⁴ and is given by

$$\frac{\Delta I}{I_0} = \left\{ \frac{1}{6} + \frac{2}{P_0(q)} \left[\frac{\sin(qL)}{(qL)^3} - \frac{1}{(qL)^2} \right] \right\} \frac{\Delta\alpha_{\text{el}}E^2}{2k_{\text{B}}T} \quad (11)$$

The prefactor is determined by the length of a rod and the scattering vector q .

3. Experimental Section

3.1. Materials. A stock solution (9.3 mg/mL) of fd-virus particles was prepared with the help of Prof.

Rashed (University of Konstanz) following the method of Marvin et al.²⁵ *Escherichia coli* bacteria were infected with the fd-virus. After 8 h at 37 °C the fd-virus bred rapidly by a factor 1000. The reproduction was stopped and the virus was separated from the bacteria by several steps of precipitation and centrifugation. Finally, the fd-virus suspension was ultracentrifuged in a CsCl gradient and dialyzed against deionized water to obtain a pure stock solution. The samples were prepared by diluting the stock solution with highly purified water ($R = 18 \text{ M}\Omega$). The actual particle concentration of a sample was determined by the characteristic UV absorption. The extinction coefficient of the fd-particles in their absorption maximum at $\lambda = 269 \text{ nm}$ is $\epsilon = 3.84 \text{ cm}^2/\text{mg}$ (cell length = 1 cm). The absorption was measured using a Beckmann spectrometer (DU-64, Darmstadt, Germany).

We add some remarks on the flexibility of the fd-virus particles to clarify that in the scope of this work (low salt conditions) the flexibility of the fd-phage is negligible. In a recent publication of Johnner et al.²⁶ the more flexible polyelectrolyte NaPSS is examined at very low ionic strengths. With decreasing ionic strength the flexibility of NaPSS chains decreases enormously, and short chains can be regarded as almost stiff rods at minimal ionic strength. This shows that under low-salt conditions the rigidity of flexible polyelectrolytes increases. Therefore the semiflexible fd-virus becomes stiffer at lower salt concentrations and its flexibility can be assumed as very small at minimal ionic strength. Flexibility greatly complicates birefringence analysis; however effects due to such a small flexibility are within the experimental error. The rigidity of the fd-virus at minimal ionic strength is further confirmed by the monoexponential decay of the birefringence signal after the electric field is switched off.^{29,30} In addition, according to Maeda and Fujime²⁰ the persistence length of the fd-virus is more than double its contour length and increases under low-salt conditions. The influence of this small flexibility on the form factor $P(q)$ within the light scattering regime ($qL \leq 30$) is even negligible considering the value of Maeda and Fujime at higher ionic strength. This can be seen by applying the results of the theory for wormlike chains near the rodlike limit published by Norisuye et al.²⁷

3.2. Magnetic Birefringence. In the magnetic birefringence apparatus the quartz cells, which contain the suspension, have a path length of 0.5 cm to avoid wall effects. Mixed-bed-ion-exchange-resin (MB3, Serva Diagnostics, Heidelberg, Germany) was added to the samples to reach minimal ionic strength. The cells were placed in a temperature-stabilized (20 ± 0.1 °C) sample holder in a Bitter type magnet (maximum field 16.8 T), which had a small radial bore. The magnetic birefringence Δn_0 was measured with good sensitivity (resolution $\Delta n_0 \approx 10^{-9}$, wavelength $\lambda = 632.8 \text{ nm}$) using a combined photoelastic modulation and compensation technique which is described elsewhere.²⁸ Polarizer and analyzer are crossed and at 45° with respect to the magnetic field direction. A small 50 kHz modulation of the birefringence is produced by a photoelastic modulator, resulting in a 100 kHz intensity modulation of the photodiode output. Any superimposed steady-state (magnetic) birefringence produces an additional 50 kHz photodiode output which is phase sensitively detected, dc-converted, and used (as error signal in a feedback loop) to compensate the steady-state birefringence by means of a Pockels cell. Hence, in the

compensated case the voltage across the Pockels cell is a direct measure of the magnetic birefringence Δn_0 .

3.3. Electric Birefringence. The electric birefringence apparatus is a commercial instrument (spectrometer DB10, Suck, Siegen, Germany) and similar to that described elsewhere.^{17,29,30} The birefringence was measured at the wavelength of 632.8 nm in quartz cells with $l = 5 \text{ cm}$ path length. The cell is temperature stabilized at 20 ± 0.1 °C and placed between the polarizer, $\lambda/4$ -plate, and analyzer. The polarizer and analyzer are crossed and at 45° with respect to the electric field direction. The intensity of the transient birefringent sample is detected by a photomultiplier. The intensity is given by

$$i \propto i_0 \sin^2\left(\alpha + \frac{\delta}{2}\right) \quad (12)$$

where i_0 is the intensity of the incident light, α is the angle of the analyzer turned out of the crossed position with respect to the polarizer and δ is the phase shift proportional to the steady-state birefringence: $\delta = 2\pi l \Delta n_0 / \lambda$. The electric field is applied for $\alpha = 0^\circ$, and the transient change of intensity is recorded. The birefringence is obtained in the absence of an electric field for an optically isotropic suspension ($E = 0$) by turning the analyzer until the same intensity as in the case of an optically anisotropic sample ($E \neq 0$) is detected. According to eq 12 the resulting α is directly related to the birefringence Δn_0 . At a electrode distance of 2.5 mm a maximum electric field strength of $1.6 \times 10^5 \text{ V/m}$ can be achieved.

3.4. Light Scattering Apparatus. For the static light-scattering investigations a light-scattering apparatus (ALV, Langen, Germany) was used consisting of a computer-controlled goniometer table with focusing and detector optics, a power-stabilized 3 W argon laser (Spectra Physics), a digital photon counter, and a temperature control which stabilizes the temperature of the sample at $T = 20 \pm 1$ °C. A light-scattering cell¹³ was constructed with circular platinum electrodes (radius = 7 mm; electrode distance = 1–1.5 mm) providing a homogeneous electric field in the scattering volume. The electric field is perpendicular to the observation plane. The cell is coupled to a tube system described in section 3.5. The electric pulse sequences (square wave) are generated by a function generator and amplified by two wideband Krohn-Hite amplifiers (Model 7500, Avon, USA). At an electrode distance of 1 mm a maximum electric field strength of $4 \times 10^5 \text{ V/m}$ can be achieved. The length of a pulse sequence was chosen long enough to attain a steady-state value of the measured intensity and ranged between 100 and 300 ms. Measurements, field generation, and data acquisition are controlled by a personal computer. Intensity data are corrected by the dark rate of photomultiplier and by the angle dependence of the scattering volume. The magnitude of the scattering vector ranges from 2.4×10^{-2} to $3.3 \times 10^{-2} \text{ nm}^{-1}$ at a laser wavelength of $\lambda = 488 \text{ nm}$ in aqueous solution with a refractive index of $n_s = 1.33$.

3.5. Tube System. In a closed circuit including either the electric birefringence or the electric field light-scattering cell the samples were deionized by pumping them with a tube pump through mixed-bed-ion-exchange-resin (MB3, Serva Diagnostics, Heidelberg, Germany) until the minimal ionic strength was achieved.³¹ The ionic strength depends on the particle concentration. At minimal ionic strength the suspension can be considered

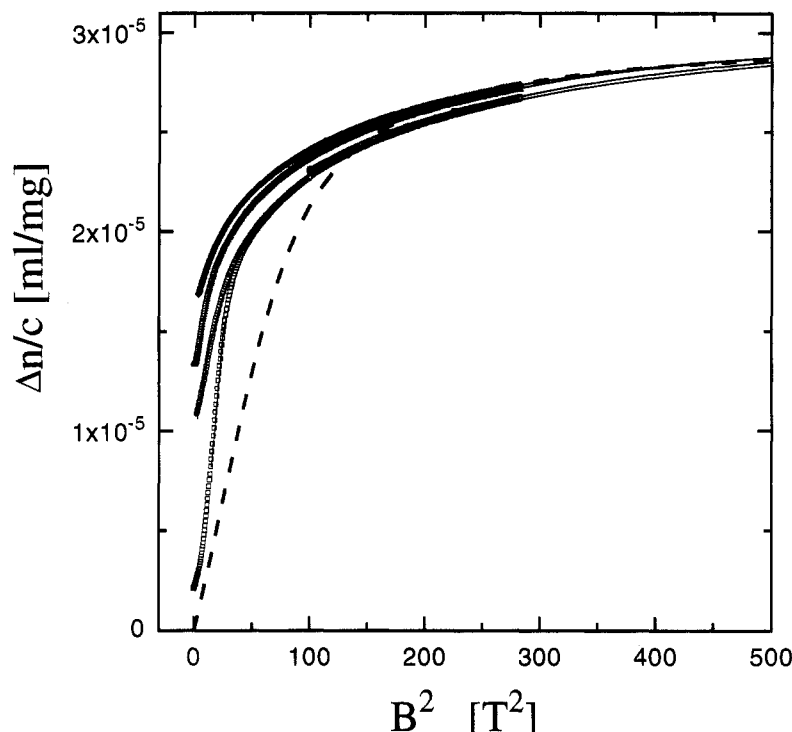


Figure 1. Magnetic field dependent specific birefringence of an fd-virus suspension of 0.8 mg/mL at minimal ionic strength. The measured specific birefringence (open symbols), the fits according to eq 13 (solid lines), and the order parameter (dashed line) are plotted.

free of small ions other than H^+ and OH^- . The conductivity of the suspension was measured with a Knick conductometer (Knick, Berlin, Germany) in a conductivity cell (LA01, WTW, Weilheim, Germany) coupled to the tube system.

4. Results and Discussion

4.1. Magnetic Birefringence. The saturation value of the birefringence Δn_{sat} is determined in a magnetic birefringence experiment. Aqueous fd-virus suspensions with a particle concentration of 0.8 mg/mL and minimal ionic strength are examined. In the thermal equilibrium at a temperature of 20 °C the samples are optically anisotropic, indicating a liquid crystalline phase. If the sample is shaken, the birefringence disappears and the sample becomes optically isotropic. The isotropic sample is put in the magnetic birefringence apparatus, where it starts recrystallizing and a remnant birefringence signal is detected. Now the magnetic field is swept from $B = 0$ T to $B = 16.8$ T in 400 s. The birefringence increases with the magnetic field strength and shows strong evidence of saturation at $B = 16.8$ T. At constant field strength of 16.8 T the birefringence signal remains constant. Even at this high magnetic field strength we could not reach the saturation plateau, a similar behavior is found by Tang and Fraden.⁹ After the field was swept down again to $B = 1$ T, the sample had a strong remnant birefringence, indicating its liquid crystalline character. Repeating the upsweeps to $B = 16.8$ T leads to slightly higher birefringence values as in the first sweep, while the measured values remain constant after the fifth sweep. The downsweeps to $B = 1$ T were done three times and show an increasing remnant birefringence after each sweep.

We focus our interest on the saturation value of the magnetic birefringence Δn_{sat} . To determine this value, we compared the measured birefringence (open symbols) with the order parameter (dashed line) defined in eq 3

and fitted the data by the following function (solid lines), as shown in Figure 1:

$$\Delta n = \Delta n_{\text{sat}} \left(1 - |a_1| e^{-B^2/\tau} - \frac{|a_2|}{B^2 - |a_3|} \right) \quad (13)$$

where a_1 , a_2 , a_3 , τ , and Δn_{sat} are fit parameters. This yields a saturation value of $\Delta n_{\text{sat}}/c = (3.0 \pm 0.3) \times 10^{-5}$ mL/mg.

At low fields the order parameter deviates significantly from the measured data. This is not surprising since the order parameter solely expresses the mean interaction of one particle with an external field. In our case the strong interparticle correlation leads to liquid crystalline domains which are oriented in the field. The existence of the liquid crystalline domains is seen in the remnant birefringence at $B = 0$ T. After the experiments in the magnetic field the birefringence observed between crossed polarizers is homogeneous all over the sample. This is evidence for a nematic phase, as is also found by Tang and Fraden⁹ at higher particle concentrations. At higher magnetic fields the birefringence is described by the order parameter and the saturation value can be extrapolated. The data are fitted well by the function given by eq 13, which in the high-field limit has the same asymptotical behavior as the order parameter³² and provides the same saturation value Δn_{sat} . In spite of the good agreement of the saturation value a physical interpretation of the exponential term describing the low-field behavior in the fit function is still lacking.

The existing literature value of $\Delta n_{\text{sat}}/c = 6 \times 10^{-5}$ mL/mg was determined by Torbet and Maret⁴ with a sample of an fd-particle concentration of 16.2 mg/mL in 10 mM Tris-HCl. A second value of $\Delta n_{\text{sat}}/c$ in the range 2.4×10^{-5} to 2.7×10^{-5} mL/mg for an fd-virus concentration of 12 mg/mL and an ionic strength of 23 mM can be extrapolated from the data of Tang and Fraden.⁹ The

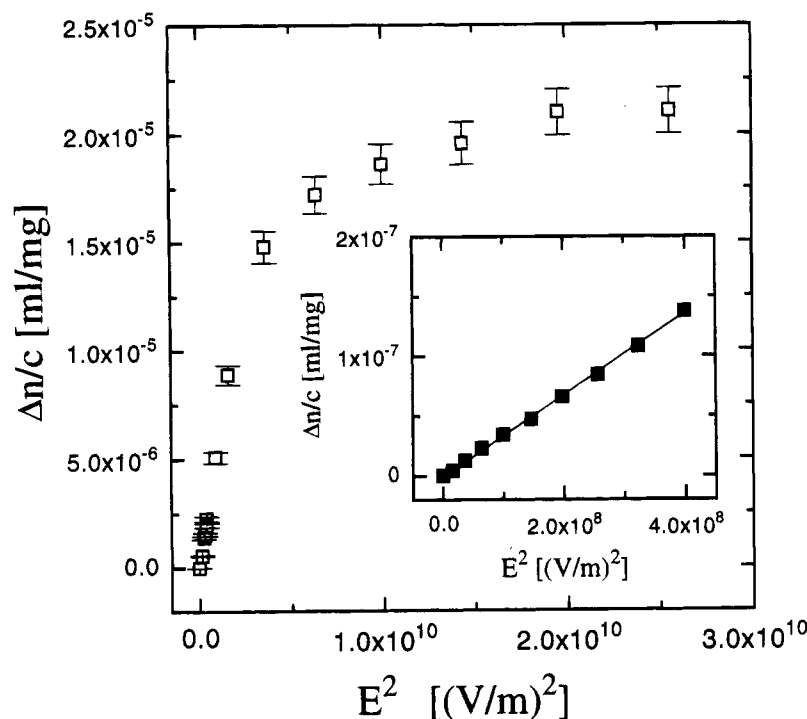


Figure 2. Electric field dependent specific birefringence of an fd-virus suspension of 0.021 mg/mL at minimal ionic strength: (a) electric field frequency of 10 kHz; (b) Kerr behavior at an electric field frequency of 3 kHz.

discrepancy of the above values measured at similar concentrations and ionic strengths is inconsistent and needs clarification. Therefore we also measured the saturation value $\Delta n_{\text{sat}}/c$ in a high magnetic field, however for a sample within our experimental conditions, i.e. at a low particle concentration of 0.8 mg/mL and minimal ionic strength (respectively strong interparticle interaction). In comparison of our value of $\Delta n_{\text{sat}}/c$ with the value estimated from the examinations by Tang and Fraden,⁹ no significant concentration dependence is observed within experimental error. If the fd-particles are aligned completely parallel to the field, the saturation value $\Delta n_{\text{sat}}/c$ is expected to be independent of the particle concentration because $\Delta n_{\text{sat}}/c$ is determined by the optical anisotropy $\Delta \alpha_{\text{opt}}$ of a single fd-particle,⁴ i.e. the difference of the optical polarizabilities parallel and perpendicular to the rod axis.

4.2. Electric Birefringence. An aqueous fd-virus suspension with a particle concentration of $c = 0.021$ mg/mL at minimal ionic strength corresponding to a conductivity of $0.36 \mu\text{S/cm}$ is examined. At a temperature of 20°C the sample is optically isotropic ($E = 0$). The measurements are performed in pulsed square wave electric fields. Figure 2 shows the field strength dependent birefringence Δn_0 at a field frequency of 10 kHz. A saturation occurs at an electric field strength of about 1.4×10^5 V/m. The saturation value is 30% smaller than the value $\Delta n_{\text{sat}}/c$ obtained in the magnetic birefringence experiment. An explanation for this deviation is a stripping of the counterion cloud in high electric fields, as was suggested in a previous paper.⁶

Since the electro-optic effect (Δn and $\Delta I/I_0$, respectively) depends on the frequency of the electric field,^{6,13} the electric anisotropy $\Delta \alpha_{\text{el}}$ is also frequency dependent. $\Delta \alpha_{\text{el}}$ is determined from the Kerr behavior in the electric birefringence experiment using the saturation value of our magnetic birefringence examination (eq 6). In the Kerr regime at a low degree of particle orientation the maximum of the electro-optic effect is found at about 2–3 kHz.^{6,13} Therefore the electric anisotropy $\Delta \alpha_{\text{el}} =$

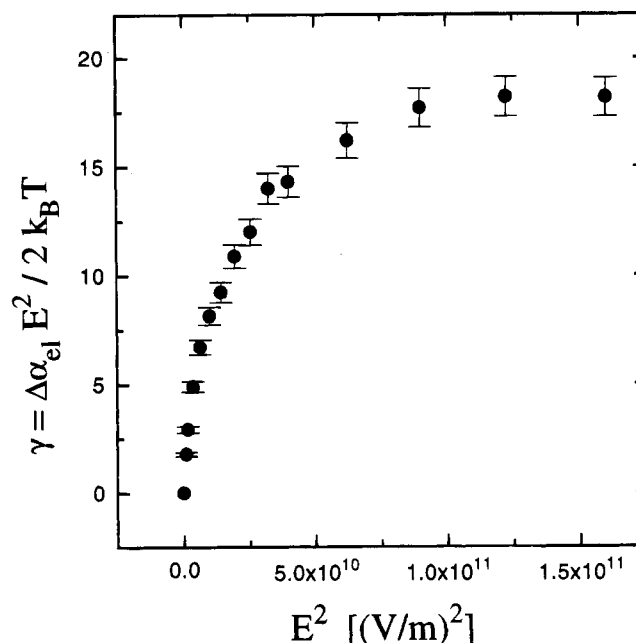


Figure 3. Electric field dependence of γ for an fd-virus suspension of 0.026 mg/mL at a field frequency of 10 kHz and minimal ionic strength.

$(1.8 \pm 0.2) \times 10^{-29} \text{ F m}^2$ at 3 kHz is somewhat larger than at $f = 10$ kHz $\Delta \alpha_{\text{el}} = (1.2 \pm 0.2) \times 10^{-29} \text{ F m}^2$. However at higher field strengths the frequency behavior of the electro-optic effect deviates from that at a low degree of particle orientation and the dispersion maximum shifts to higher frequencies of approximately 10–20 kHz.¹³ A qualitative explanation of the maximum shift is suggested in ref 13. In order to achieve maximum particle alignment in an external electric field a frequency of 10 kHz was applied (see Figures 2 and 3).

4.3. Electric Field Light Scattering. In an electric field light-scattering experiment the relative change of the scattered light $\Delta I/I_0$ is detected. To examine the

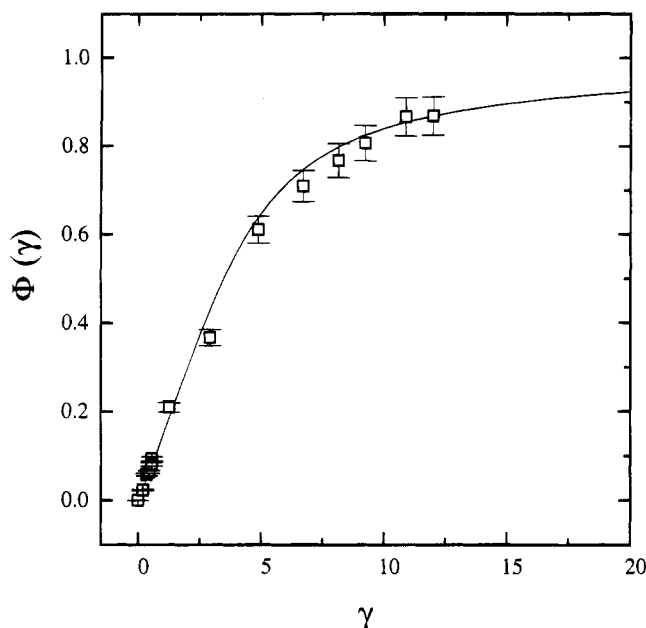


Figure 4. Order parameter $\Phi(\gamma)$. The theoretically calculated order parameter (solid line) and the experimental order parameter for the data of Figure 2 (open symbols) are plotted.

electric anisotropy $\Delta\alpha_{el}$, the scattering angle is fixed at 140° and an alternating electric field of 3 kHz is applied. $\Delta\alpha_{el}$ is determined from the slope of the linear part of the saturation curve $\Delta I/I_0(E^2)$, the scattering angle, and the particle length. We calculate the electric anisotropy $\Delta\alpha_{el}$ for three different samples with a particle concentration of 0.02 mg/mL at minimal ionic strength (eq 11). A mean value of $\Delta\alpha_{el} = (1.8 \pm 0.2) \times 10^{-29} \text{ F m}^2$ is obtained, which is in good agreement with the electric anisotropy $\Delta\alpha_{el}$ determined by the electric birefringence measurement using our magnetic saturation value Δn_{sat} (eq 6). This is an independent confirmation of our magnetic birefringence saturation value of $\Delta n_{sat}/c = 3 \times 10^{-5} \text{ mL/mg}$.

Further we examine the change of the scattered light $\Delta I/I_0$ for a suspension with a particle concentration of 0.026 mg/mL at minimal ionic strength as a function of the scattering angle for various electric field strengths. To achieve maximum particle alignment at high electric fields, a frequency of 10 kHz is applied. We compare the measured data of $\Delta I/I_0$ with the theoretical treatment of Stoimenova given in eq 10 at scattering angles above 100° , where interparticle correlations can be neglected.¹³ This yields the electric anisotropy $\Delta\alpha_{el}(E)$ and $\gamma(E)$, respectively, for the different electric field strengths shown in Figure 3. In the Kerr regime ($\gamma \leq 1$) γ is proportional to E^2 and $\Delta\alpha_{el}(E) = \text{constant}$. For $\gamma > 1$ the electric anisotropy $\Delta\alpha_{el}(E)$ decreases with increasing electric field strength. At high electric field strengths γ remains constant, corresponding to a decrease of $\Delta\alpha_{el}(E) \propto E^{-2}$. According to the order parameter in Figure 4 the maximum experimental value of $\gamma(E \geq 2.5 \times 10^5 \text{ V/m}) \approx 18$ indicates a deviation of about 10% of complete particle alignment along the electric field.

We have shown in a previous paper⁶ that the electric anisotropy of an fd-virus particle mainly depends on the polarization of its counterion cloud. A decrease of $\Delta\alpha_{el}(E)$ with increasing field strengths is theoretically explained by several authors^{10–12} with a stripping of the counterions away from the electrostatic influence of the central rod. For this effect a decrease of $\Delta\alpha_{el}(E) \propto E^{-2}$

is predicted at high electric fields,¹⁰ leading to a maximum value of γ and therefore an incomplete orientation of the suspended particles even at very high electric fields. For the first time we measured such a decrease of $\Delta\alpha_{el}(E)$. This could explain the significant deviation of the electric saturation value from the saturation value obtained in the magnetic field.

From the electric field light-scattering results the dependence of the field parameter γ on the electric field strength is known (Figure 3); therefore we can deduce the electric birefringence as a function of γ . According to eq 5 $\Delta n_0(\gamma)$ is related to the saturation value Δn_{sat} and the order parameter $\Phi(\gamma)$ which is solely determined by γ . The saturation value of the electric birefringence signal $\Delta n_0(E = 1.6 \times 10^5 \text{ V/m})/c = 2.1 \times 10^{-5} \text{ mL/mg}$ corresponds to $\gamma(E = 1.6 \times 10^5 \text{ V/m}) = 12$ and to a value of the order parameter of $\Phi(\gamma = 12) = 0.87$ (see Figure 4), and according to eq 5 a saturation value for the electric birefringence of $\Delta n_{sat}/c = \Delta n_0(E = 1.6 \times 10^5 \text{ V/m})/(c\Phi(\gamma = 12)) = 2.4 \times 10^{-5} \text{ mL/mg}$ is obtained. Figure 4 shows the theoretical order parameter $\Phi(\gamma)$ and the measured order parameter, $\Phi_{exp}(\gamma) = \Delta n_0(\gamma)/\Delta n_{sat}$, using this saturation value of $2.4 \times 10^{-5} \text{ mL/mg}$. A good agreement is found which indicates a pure induced dipole moment orienting the particles.

In spite of the correction due to the stripping effect the saturation value $\Delta n_{sat}/c$ in the magnetic birefringence experiment is 20% higher than the saturation value $\Delta n_{sat}/c$ obtained in the electric birefringence experiments. This discrepancy seems to be out of experimental error; an explanation could be a slight change in the conformation of the coat proteins of the fd-virus in high electric fields resulting in a decrease of the optical anisotropy $\Delta\alpha_{opt}$ of a single rod.⁴

5. Conclusions

The orientation behavior of rodlike fd-virus particles in an aqueous suspension of very low ionic strength (10^{-6} M) in external electric and magnetic fields has been examined. The rodlike fd-virus particles were aligned in a magnetic birefringence experiment. At a field of $B = 16.8 \text{ T}$ evidence of saturation of the birefringence is observed for a nematic liquid crystalline sample of particle concentration $c = 0.8 \text{ mg/mL}$. The saturation value of the birefringence is extrapolated to $\Delta n_{sat}/c = 3 \times 10^{-5} \text{ mL/mg}$. In an external electric field the particles are oriented by an induced dipole mechanism due to the anisotropic polarization of the diffuse counterion cloud. The electric anisotropy $\Delta\alpha_{el}$ measured in an electric birefringence experiment are in good agreement with the $\Delta\alpha_{el}$ determined with electric field light scattering. This is an independent confirmation of the saturation value obtained with magnetic birefringence. At higher electric fields the partly stripped away counterion cloud is related to a decreasing electric anisotropy $\Delta\alpha_{el}$ with increasing electric field strength. In electric field light-scattering examinations we measured the decrease of $\Delta\alpha_{el}(E)$ as a function of the electric field strength and found good accordance with theoretical predictions. To our knowledge this is the first experimental confirmation of the stripping effect.

Acknowledgment. This work was supported by the Deutsche Forschungsgemeinschaft (Grant SFB 306). The magnetic birefringence experiments have been carried out in the High Magnetic Field Laboratory of the Max-Planck-Institut für Festkörperphysik in Gre-

noble, and we are grateful for the support given by the personnel.

References and Notes

- (1) Frank, H.; Day, L. A. *Virology* **1970**, *42*, 144.
- (2) Newman, J.; Swinney, H.; Day, L. A. *J. Mol. Biol.* **1977**, *116*, 593.
- (3) Banner, D. W.; Nave, C.; Marvin, D. A. *Nature* **1981**, *289*, 814.
- (4) Torbet, J.; Maret, G. *Biopolymers* **1981**, *20*, 2657.
- (5) Zimmermann, K.; Hagedorn, H.; Heuck, C.; Hinrichsen, M.; Ludwig, H. *J. Biol. Chem.* **1986**, *261*, 1653.
- (6) Kramer, H.; Graf, C.; Hagenbüchle, M.; Johnner, C.; Martin, C.; Schwind, P.; Weber, R. *J. Phys. II Fr.* **1994**, *4*, 1061.
- (7) Marvin, D. A.; Wiseman, R. L.; Wachtel, E. J. *J. Mol. Biol.* **1974**, *82*, 121.
- (8) Marvin, D. A.; Pigram, W. J.; Wiseman, R. L.; Wachtel, E. J.; Marvin, F. J. *J. Mol. Biol.* **1974**, *88*, 581.
- (9) Tang, J.; Fraden, S. *Phys. Rev. Lett.* **1993**, *71*, 3509.
- (10) Rau, D. C.; Charney, E. *Macromolecules* **1983**, *16*, 1653.
- (11) Fixman, M.; Jagannathan, S. *Macromolecules* **1983**, *16*, 685.
- (12) Yoshida, M.; Kikuchi, K.; Maekawa, T.; Watanabe, H. *J. Phys. Chem.* **1992**, *96*, 2365.
- (13) Martin, C.; Weyerich, B.; Biegel, J.; Deike, R.; Johnner, C.; Klein, R.; Weber, R. *J. Phys. II Fr.*, in press.
- (14) Hagenbüchle, M.; Weyerich, B.; Deggelmann, M.; Graf, C.; Krause, R.; Maier, E.; Schulz, S.; Klein, R.; Weber, R. *Physica A* **1990**, *169*, 29.
- (15) Maier, E.; Krause, R.; Deggelmann, M.; Hagenbüchle, M.; Weber, R. *Macromolecules* **1992**, *25*, 1125.
- (16) Stoylov, S. P. *Adv. Colloid Interface Sci.* **1971**, *3*, 45–110.
- (17) Fredericq, E.; Houssier, C. *Electric Dichroism and Electric Birefringence*; Clarendon Press: Oxford, U.K., 1973.
- (18) Stoimenova, M. V. *J. Colloid Interface Sci.* **1975**, *53*, 42.
- (19) Buitenhuis, J.; Dhont, J. K. G.; Lekkerkerker, H. N. W. *J. Colloid Interface Sci.* **1993**, *162*, 19.
- (20) Maeda, T.; Fujime, S. *Macromolecules* **1985**, *18*, 2430.
- (21) Berne, B. J.; Pecora, R. *Dynamic Light Scattering*; John Wiley & Sons: New York, 1976.
- (22) Dawson, H. *Proc. London Math. Soc.* **1898**, *29*, 519.
- (23) Wippler, C. *J. Chem. Phys.* **1956**, *53*, 321.
- (24) Stoylov, S. P. *Colloid Electro-Optics*; Academic Press: New York, 1991.
- (25) Marvin, D. A.; Wachtel, E. J. *Nature* **1975**, *253*, 19.
- (26) Johnner, C.; Kramer, H.; Martin, C.; Biegel, J.; Deike, R.; Weber, R. *J. Phys. II Fr.*, in press.
- (27) Norisuye, T.; Murakama, H.; Fujita, H. *Macromolecules* **1978**, *11*, 966.
- (28) Maret, G.; Weil, G. *Biopolymers* **1983**, *22*, 2727.
- (29) Kramer, H.; Deggelmann, M.; Graf, C.; Hagenbüchle, M.; Johnner, C.; Weber, R. *Macromolecules* **1992**, *25*, 4325.
- (30) Kramer, H. Ph.D. Thesis. Hartung-Gorre Verlag, Konstanz, 1993.
- (31) Deggelmann, M.; Palberg, T.; Hagenbüchle, M.; Maier, E.; Krause, R.; Graf, C.; Weber, R. *J. Colloid Interface Sci.* **1991**, *143*, 318.
- (32) O'Konski, C. T.; Yoshioka, K.; Orttung, W. H. *J. Phys. Chem.* **1959**, *63*, 1558.

MA946057L